



# American Journal of Environment and Climate (AJEC)

ISSN: 2832-403X (ONLINE)

VOLUME 3 ISSUE 1 (2024)



PUBLISHED BY  
E-PALLI PUBLISHERS, DELAWARE, USA

## Adsorption of Ca (II), Mn (II), Fe (III), Mg (II), and Pb (II) Ions from New Valley Groundwater Using Illite and Nanoparticles

Ghada Sayed<sup>1\*</sup>, Enas M. Abou-Taleb<sup>2</sup>, Fathy A. El-Saied<sup>3</sup>

### Article Information

**Received:** November 11, 2023

**Accepted:** December 15, 2023

**Published:** December 18, 2023

### Keywords

*Illite, Nano-Illite, Clay, Heavy Metals Removal, Kinetic Isotherms, Water*

### ABSTRACT

Heavy metal pollution is a significant environmental concern due to its potential hazards. In this study, the adsorption of Ca (II), Mn (II), Fe (III), Mg (II), and Pb (II) ions from diluted aqueous solutions was investigated using both illite and nano-illite particles. The integration of illite as a natural and cost-effective material in water treatment for areas facing water pollution challenges offers a holistic solution with positive implications for the environment, economy, and public health. The multifaceted benefits of illite underscore its potential as a valuable tool in addressing water-related issues in remote and economically constrained regions. The synthesis and characterization of nano-illite were conducted through SEM, TEM, and FTIR spectroscopy. Notably, the TEM analysis revealed that the particle size of nano-illite (ranging from 2 to 4 nm) was smaller than that of illite (ranging from 20 to 30 nm). For the adsorption experiments, batch tests were performed, and the optimal conditions were determined. It was found that the highest adsorption efficiency for the studied metal ions was achieved at a pH of 7, a contact time of 60 minutes, an illite dosage of 0.4 g, and a nano-illite dosage of 0.3 g. Furthermore, the adsorption kinetics were analyzed using the pseudo-second-order kinetic model, while the adsorption isotherms were evaluated using the Langmuir model. This investigation provides valuable insights into the effective removal of heavy metal ions from aqueous solutions using illite and nano-illite particles. The results highlight the potential applicability of these adsorbents in addressing heavy metal pollution, thereby contributing to the mitigation of environmental risks associated with such contaminants.

### INTRODUCTION

Heavy metal pollution is a serious environmental hazard on a global scale (Li *et al.*, 2022). Heavy metals such as Fe and Cu help keep the body's metabolism running smoothly (Zaynab *et al.*, 2022). However, due to the toxicity and non-biodegradability of heavy metals, their presence in groundwater has produced a slew of serious environmental problems (Hoang *et al.*, 2022). Non-biodegradable heavy metals accumulate in living organisms, causing a variety of disorders affecting the human renal, neurological, hematological, and gastrointestinal systems (Hoang *et al.*, 2021). To prevent its harmful impacts, such as accumulating in water surface bodies, that is critical to adopt creative, cost-effective, and successful methods to clean up heavy metal-contaminated water before releasing it into the environment (Jawed *et al.*, 2020). Coagulation (Zhang *et al.*, 2019; Mhina *et al.*, 2020), biodegradation (Lee *et al.*, 2019; Zhao *et al.*, 2020), adsorption (liu *et al.*, 2019), advanced oxidation (Peng *et al.*, 2017), and other classic groundwater treatment technologies are applied. Adsorption is one of the best ways to treat heavy metals in water because of its benefits, such as cheap operating costs, versatile design choices, and high efficiency (Peng *et al.*, 2017; Joziane *et al.*, 2017). Clay is a popular choice for removing heavy metals due to its affordability, ecological friendliness, high adsorption capacity, and ability to function across a wide pH range

(Burakov *et al.*, 2018; Mohammad, 2017).

Recently, a variety of clay types, such as bentonite, kaolin, and illite, have been employed to purify water (Ishwah *et al.*, 2022). with high metal concentrations (Mohammad, 2017; Sari *et al.*, 2022).

Illite, a natural and cost-effective clay with small particle size and a large surface area, has been found to be particularly effective for removing heavy metals from aqueous solutions (Yuan *et al.*, 2016; Zhang *et al.*, 2016). The use of nanomaterials for water pollution remediation has gained attention for their ability to increase surface area and adsorb a range of contaminants (Anjum *et al.*, 2019). Our goal was to create an inexpensive and natural adsorbent by developing nano-illite. We then tested the cleansing capabilities of illite and nano-illite for aqueous media contaminated with Fe (III), Mn (II), Pb (II), Ca (II), and Mg (II). We thoroughly analyzed the removal efficiency of illite and nano-illite under ideal analytical conditions, such as beginning pH of the solution, contact time, initial adsorbate, and adsorbent concentration. We used isotherm, kinetic, and thermodynamic methods to model the adsorption process.

The presence of heavy metals in the groundwater of wells in the New Valley poses a significant challenge. Given the economic constraints that limit the use of high-cost techniques, exploring new, low cost-effective methods for water treatment becomes crucial. Considering the

<sup>1</sup> National Food Safety Authority, Cairo, Egypt

<sup>2</sup> Wastewater Treatment Technologies, Water Pollution Research Department, National Research Centre, EEAA Ministry of Environment, Cairo, Egypt

<sup>3</sup> Chemistry Department, Faculty of Science, Menoufia University, Shebin El-Kom, Egypt

\* Corresponding author's e-mail: [ghadasaid\\_2007@yahoo.com](mailto:ghadasaid_2007@yahoo.com)

environmental resources available, finding a low-cost adsorbent with widespread availability, high adsorption capacity, rapid removal rate, and minimal adverse effects on treated water is paramount in addressing this challenge.

## MATERIAL AND METHODS

### Study Area and Collection

The study was conducted in the city of Al-Kharga, located in the New Valley Governorate in the Western Desert of Egypt. This region relies on groundwater as a primary source of fresh water for drinking and agriculture. The water used in the experiments was collected from wells in the villages of Nasser and Boulak in the city of Al-Kharga. This choice was made due to the high concentration of heavy metals in these wells. The experiments were carried out at the Faculty of Science, Minoufiya University.

### Instruments

- pH meter (WTW-inolab in Germany),
- Flame Atomic Absorption Spectrophotometer (FAAS) (Perkin Elmer 503).
- Nicolet FT-IR spectrophotometer between 4000 and 400  $\text{cm}^{-1}$ .
- Scanning electron microscope (SEM) (JSM-5300, JEOL Ltd.). Gold was sputtered onto the SEM specimens to boost conductivity using a JEOL-JFC-1100E coating procedure.

### Chemicals

- o Analytical grade Merck, Germany chemicals;  $\text{MgCl}_2$ ,  $\text{MnCl}_2$ ,  $\text{FeCl}_3$ ,  $\text{CaCl}_2$ , and  $\text{Pb}(\text{NO}_3)_2$  were used.
- o Solutions of Mg (II), Mn (II), Fe (III), Ca (II), and Pb (II) were prepared with a concentration of 1000 mg/l.
- o Two types of adsorbents, illite and nano illite, were prepared for the study.

### Experimental

#### Preparation of Nano-Illite Clay

Hydrothermal method for nano materials preparation was used to prepare the nano-illite clay; illite clay was ground into small particles and soaked in distilled water to bring the pH of the wash water up to 7. The purified sample was dried for 24 hours at 70°C. For preparing nano illite, acid hydrolysis was performed using a 60% sulfuric acid ( $\text{H}_2\text{SO}_4$ ) solution at 45°C. for 30 minutes with continual stirring. The nano-illite was periodically washed in distilled water to maintain a constant pH level, then dried for 24 hours at 80 °C. The material was thoroughly crushed and sieved to produce a homogenous particle size (45 nm).

#### Optimal Conditions Determination

The effect of contact duration (10-120 min) was evaluated for illite and nano illite adsorbents. The pH influence was also investigated by altering the pH of solutions from 1 to 9 using 1.0 M HCl and 1.0 M NaOH. Initial concentrations and adsorbent dose had an impact in the 2-20 ppm and (0.1 - 0.5 g) ranges, respectively. The

solutions were removed using a 0.45-mm filter membrane. The remaining amounts were determined using an atomic absorption spectrometer. The elimination percentage and adsorption capacity were determined using the equations S1 and S2 in the supplementary materials. (Kwon *et al.*, 2010).

The pseudo-first order (Eq. S3) and pseudo-second order (Eq. S4) equations were used to simulate the kinetics of adsorption onto illite and nano-illite. Adsorption isotherms were investigated utilizing the Langmuir and Freundlich isotherms (Eqs. (S5) and (S6)).

High purity chemicals from Merck, Germany were used in this study without further purification. Solutions of Mg (II), Mn (II), Fe (III), Ca (II), and Pb (II) were prepared with a concentration of 1000 mg metal ions/L by using  $\text{MgCl}_2$ ,  $\text{MnCl}_2$ ,  $\text{FeCl}_3$ ,  $\text{CaCl}_2$ , and  $\text{Pb}(\text{NO}_3)_2$ , respectively. The pH values of these solutions were measured using a pH meter (WTW-inolab in Germany), and the residual concentrations were determined using a Flame Atomic Absorption Spectrophotometer (FAAS) (Perkin Elmer 503). The most functional groups were identified by the KBr pellet method on a Nicolet FT-IR spectrophotometer between 4000 and 400  $\text{cm}^{-1}$ . Surface size was assessed by using a scanning electron microscope (SEM) (JSM5300, JEOL Ltd.). Gold was sputtered onto the SEM specimens to boost conductivity using a JEOL-JFC-1100E coating procedure.

Two types of adsorbents, illite and nano illite, were prepared for the study. Illite was ground into small particles and soaked in distilled water to bring the pH of the wash water up to 7. The purified sample was dried for 24 hours at 70°C. For preparing nano illite, acid hydrolysis was performed using a 60% sulfuric acid ( $\text{H}_2\text{SO}_4$ ) solution at 45 degrees Celsius for 30 minutes with continual stirring. The nano-illite was periodically washed in distilled water to maintain a constant pH level, then dried for 24 hours at 80 °C. The material was thoroughly crushed and sieved to produce a homogenous particle size (45 m).

The effect of contact duration (10-120 min) was evaluated for illite and nano illite adsorbents. The pH influence was also investigated by altering the pH of solutions from 1 to 9 using 1.0 M HCl and 1.0 M NaOH. Initial concentrations and adsorbent dose had an impact in the 2-20 ppm and (0.1 - 0.5 g) ranges, respectively. The solutions were removed using a 0.45-mm filter membrane. The remaining amounts were determined using an atomic absorption spectrometer. The elimination percentage and adsorption capacity were determined using the equations S1 and S2 in the supplementary materials.

The pseudo-first order (Eq. S3) and pseudo-second order (Eq. S4) equations were used to simulate the kinetics of adsorption onto illite and nano-illite. Adsorption isotherms were investigated utilizing the Langmuir and Freundlich isotherms (Eqs. (S5) and (S6)).

## RESULTS AND DISCUSSIONS

Characterization of Illite and nano illite

**Transmission Electron Micrograph (TEM)**

Transmission electron micrographs of the two adsorbents showed that nano illite particles were smaller than illite

nanoparticles (2–4 nm in size), as well as more spherical, homogenous, and mono-dispersed (20 to 30 nm).

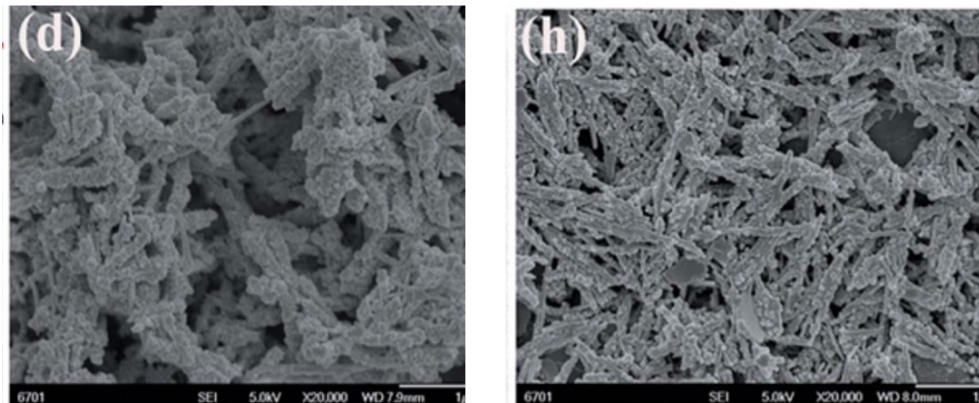


Figure 1: TEM image of d) illite and h) nano-illite.

**Scanning Electron Micrograph (SEM)**

SEM micrographs were used to analyze the surface morphology of illite and nano-illite. The scanning

electron micrograph (SEM) of the surface demonstrated the presence of irregularly formed pores that are well-suited for adsorbing metal ions from solutions.

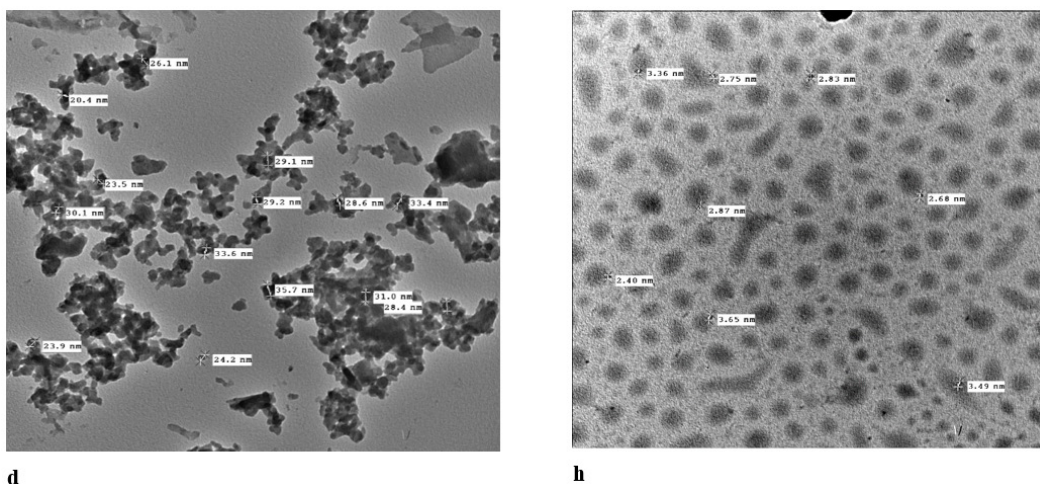


Figure 2: SEM image of d) illite and h) nano-illite.

**Fourier Transform InfraRed Spectrophotometer (FTIR)**

FTIR was used to determine the composition of the

surface's functional groups. Aluminum phyllosilicate, often known as illite, was identified. The accompanying peaks originated from the OH- bending at 912 cm<sup>-1</sup>,

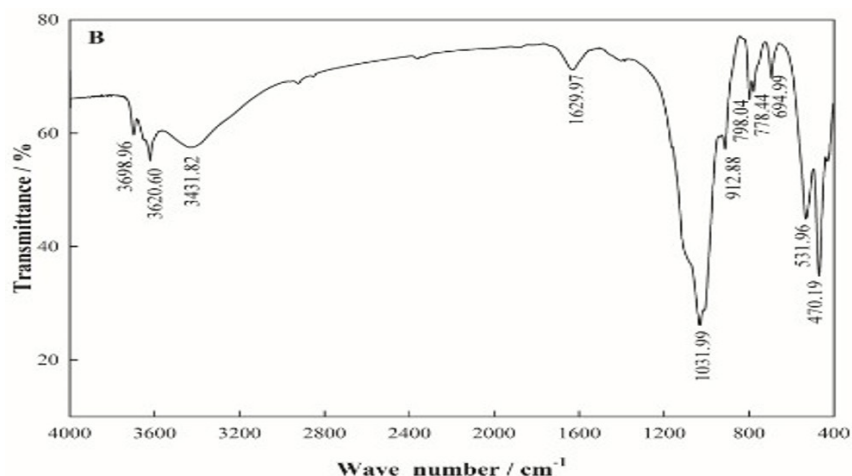


Figure 3: FTIR spectrum of adsorbents

which was determined to be Al-OH. Bands at 531 and 470  $\text{cm}^{-1}$  were interpreted as representing the Si-O-Al and Si-O-Si bending vibrations, respectively, while the band at 1031  $\text{cm}^{-1}$  was seen as representing the Si-O stretching vibration that is unique to the tetrahedral Si-O structure. Absorption bands at 3431 and 1629  $\text{cm}^{-1}$  were found to represent the OH- stretching and bending vibrations of the adsorbed water molecules on the clay surfaces. Adsorption of heavy metals showed a decrease in the concentration of heavy metals using the adsorption technique illite-based.

### Adsorption Mechanism (Figure 4)

#### Calcium (Ca)

##### Impact of pH

The adsorption percentages of calcium ions (Ca (II)) were investigated under different pH conditions using illite and nano-illite as adsorbents. Illite exhibited exceptional performance, achieving a removal rate of 99.0% for Ca (II) at pH 7, 25°C, and a contact time of 60 minutes. Moreover, nano-illite demonstrated complete removal of calcium ions under the same conditions.

Clay minerals possess an electronegative charge, making them attractive to cationic contaminants that concentrate on their surfaces via electrostatic forces. As pH levels rise, clay becomes more electronegative due to the deprotonation of hydroxyls. Conversely, at low pH values, protonation of hydroxyls occurs due to a high concentration of  $\text{H}^+$  ions, reducing the negative charge on the surface of clay. Additionally, the abundance of  $\text{H}^+$  ions competes with cationic contaminants for adsorption sites. At pH values over 7.0, metal ion hydroxyl complexes may form, limiting action by blocking surface moieties and decreasing adsorption efficiency (Wadhawan *et al.*, 2020).

##### Impact of Adsorbent Dose

The influence of adsorbent dosage on calcium ion removal was explored. However, specific percentages for Ca (II) removal using illite were not provided in the study. Increases in adsorbent dosage often result in enhanced removal (Sen *et al.*, 2011) due to the increased availability of reactive adsorption sites.

##### Impact of Contact Time

The time-dependent adsorption behavior of calcium ions was investigated for both illite and nano-illite. Illite efficiently removed 43% of Ca (II) within the first 20 minutes, reaching complete elimination within an hour at pH 7, 25°C, and a contact time of 60 minutes. Similarly, nano-illite removed 46% of Ca (II) within the first hour, with complete elimination observed within the same timeframe.

The metal ion elimination percentage increased as the contact time increased because more surface sites were available earlier in the sorption process. However, it becomes difficult to claim the last available surface areas over time as saturation occurs (Igberase *et al.*, 2017).

These findings underscore the significant efficacy of illite and nano-illite in adsorbing calcium ions under various experimental conditions, emphasizing their potential as effective adsorbents for calcium removal in water treatment applications.

#### Impact of Heavy Metal Concentration

The study investigated the effect of heavy metal concentration, Figures 4 illustrate a decrease in initial calcium ion concentration corresponds to an increase in elimination percentage. This trend was consistent for both illite and nano-illite under conditions of 25°C, a contact time of 60 minutes, pH 7, and a specific adsorbent dose (Mg=0.3, Pb=0.2, Ca=0.4, Mn=0.4, Fe=0.3).

The observed phenomenon is attributed to the greater availability of adsorption sites at lower concentrations, facilitating rapid contaminant removal. Illite achieved a notable 99% adsorption efficiency, while nano-illite demonstrated complete removal (100%) of calcium ions at the initial concentration of  $\text{Co}=3\text{mg/L}$ .

This is due to the greater number of adsorption sites available at lower concentrations, which allows for rapid removal of contaminants. As the concentration rises, the likelihood of contact with adsorption sites increases, filling available spaces quickly. However, adsorbents have a limited capacity, resulting in remaining contaminants in the solution (Ngulube *et al.*, 2017).

#### Manganese Mn (II)

Illite exhibited the highest removal rate, reaching 99.06% at pH 7, 25°C, 60 min, with a dose of (Mg=0.3, Pb=0.2, Ca=0.4, Mn=0.4, Fe=0.3), and concentration = 3ppm.

Nano-Illite showed a removal of 60% at pH 7, 25°C, 60 min, with the same dose and concentration.

#### Iron Fe (III)

Illite demonstrated the highest removal rate, reaching 99.50% at pH 7, 25°C, 60 min, with a dose of (Mg=0.3, Pb=0.2, Ca=0.4, Mn=0.4, Fe=0.3), and concentration = 3ppm.

Nano-Illite showed a removal of 54% at pH 7, 25°C, 60 min, with the same dose and concentration.

#### Magnesium Mg (II)

Illite exhibited the highest removal rate, reaching 99.29% at pH 7, 25°C, 60 min, with a dose of (Mg=0.3, Pb=0.2, Ca=0.4, Mn=0.4, Fe=0.3), and concentration = 3ppm.

Nano-Illite showed a removal of 54% at pH 7, 25°C, 60 min, with the same dose and concentration.

#### Lead Pb (II)

Illite demonstrated the highest removal rate, reaching 99.33% at pH 7, 25°C, 60 min, with a dose of (Mg=0.3, Pb=0.2, Ca=0.4, Mn=0.4, Fe=0.3), and concentration = 3ppm.

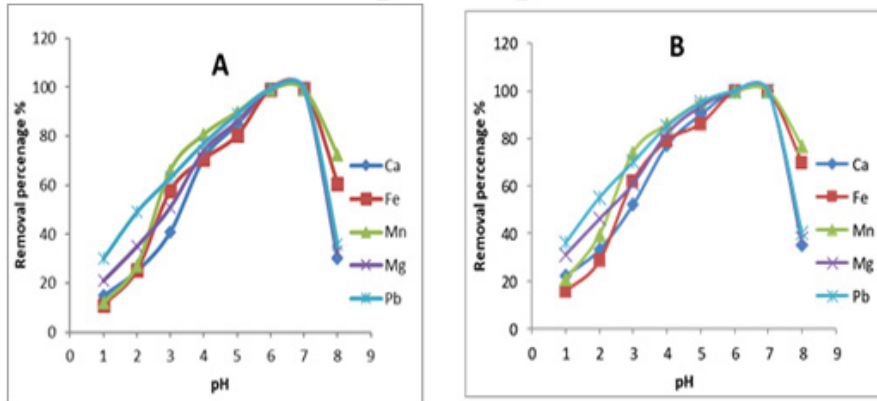
Nano-Illite showed a removal of 43% at pH 7, 25°C, 60 min, with the same dose and concentration.

**Key Observations**

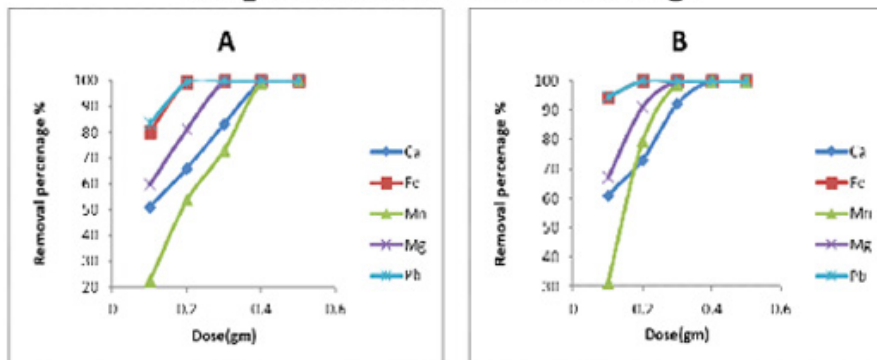
For all metal ions, Illite proved to be more efficient in removal than Nano-Illite. The removal efficiency benefited from the adsorbent dosage and the elimination percentages were affected by contact duration, whereas Nano-Illite exhibited a notable reduction but removal

effectiveness decreased with greater concentrations; initial concentration and removal % correlated inversely. At the initial  $Co=3$  mg/L concentration, both Illite and Nano-Illite demonstrated outstanding removal efficiency (99% and 100%, respectively) for all metal ions.

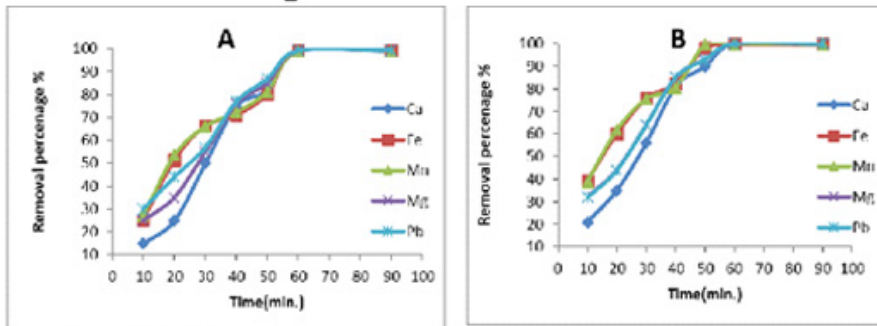
**Impact of pH**



**Impact of adsorbent dosage**



**Impact of contact time**



**Impact of adsorbent conc**

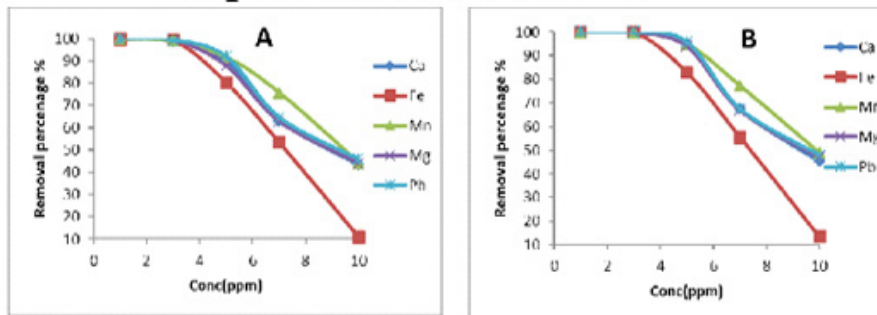
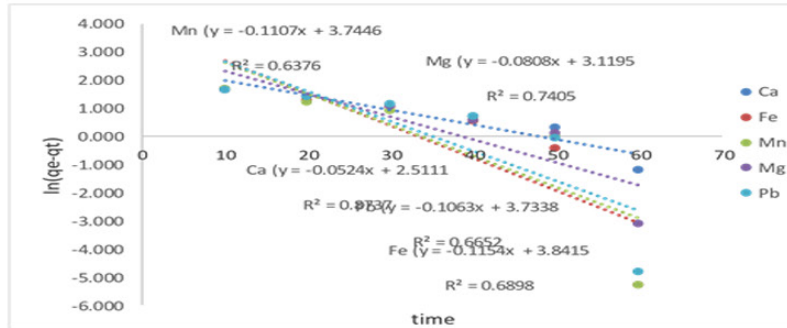


Figure 4: Adsorption mechanism (A) illite and (B) nanoillite

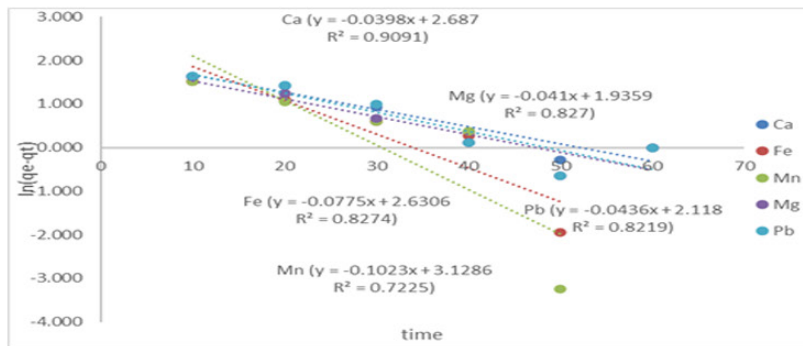
**Adsorption Kinetics**

To ensure the success of the procedure, understanding the adsorption mechanism is crucial. This can only be achieved by studying the adsorption kinetics (Silva *et al.*, 2004). To identify the most appropriate model, the

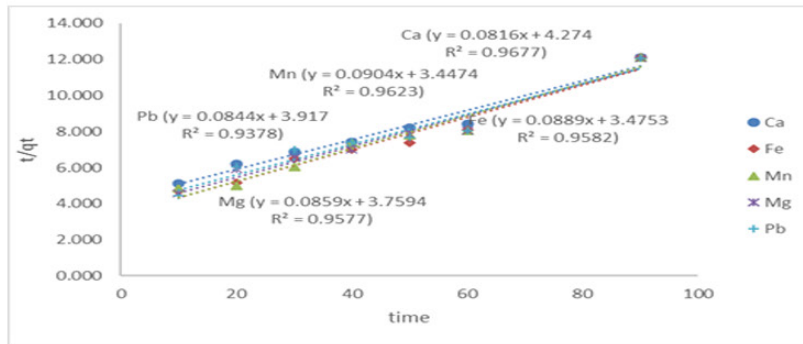
kinetics of cation adsorption were investigated with varying contact periods. Tables 1 and 2 present the relevant data, while Figures 5 depict the pseudo-1st order and pseudo-2nd-order models for the ions. (Langmuir, 1918)



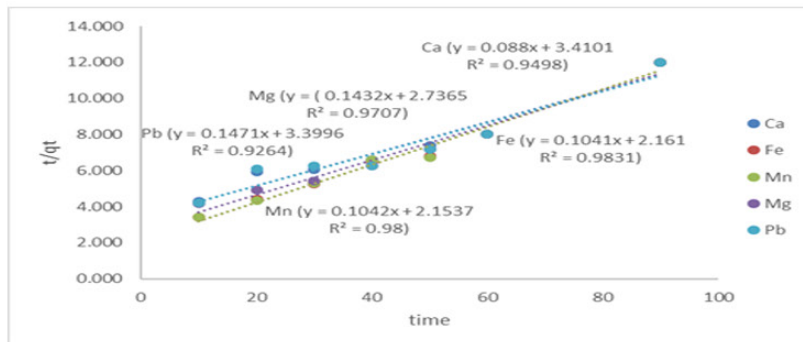
**Model of Pseudo-1<sup>st</sup>-order on illite**



**Model of Pseudo-1<sup>st</sup>-order on Nano illite**



**Model of Pseudo-2<sup>nd</sup>-order on illite**



**Model of Pseudo-2<sup>nd</sup>-order on Nano illite**

**Figure 5:** pseudo-1st order and pseudo-2nd-order models for the ions

**Table 1:** Calculated parameters of kinetic models on illite

Pseudo-first-order	Parameters	Ca <sup>2+</sup>	Mn <sup>2+</sup>	Fe <sup>3+</sup>	Mg <sup>2+</sup>	Pb <sup>2+</sup>
	k <sub>1</sub> (min <sup>-1</sup> )	0.0524	0.1107	0.1154	0.0808	0.1063
	qe cal.(mg/g)	12.318	42.292	46.595	22.635	41.837
	R2	0.8737	0.6376	0.6898	0.7405	0.6652
Pseudo-second-order	Parameters	Ca <sup>2+</sup>	Mn <sup>2+</sup>	Fe <sup>3+</sup>	Mg <sup>2+</sup>	Pb <sup>2+</sup>
	k <sub>2</sub> (g/mg min)	0.00155	0.00237	0.00227	0.00195	0.00181
	qe cal.(mg/g)	12.254	11.061	11.248	11.641	11.848
	R2	0.9677	0.9623	0.9582	0.9577	0.9378
Experimental	Parameters	Ca <sup>2+</sup>	Mn <sup>2+</sup>	Fe <sup>3+</sup>	Mg <sup>2+</sup>	Pb <sup>2+</sup>
	qe Exp.(mg/g)	7	7	7	7	7

**Table 2:** Calculated parameters of kinetic models on illite

Pseudo-first-order	Parameters	Ca <sup>2+</sup>	Mn <sup>2+</sup>	Fe <sup>3+</sup>	Mg <sup>2+</sup>	Pb <sup>2+</sup>
	k <sub>1</sub> (min <sup>-1</sup> )	0.0398	0.1023	0.0775	0.041	0.0436
	qe cal.(mg/g)	14.687	22.841	13.882	6.930	8.314
	R2	0.9091	0.7225	0.8274	0.827	0.8219
Pseudo-second-order	Parameters	Ca <sup>2+</sup>	Mn <sup>2+</sup>	Fe <sup>3+</sup>	Mg <sup>2+</sup>	Pb <sup>2+</sup>
	k <sub>2</sub> (g/mg min)	0.0023	0.0005	0.00501	0.0075	0.0064
	qe cal.(mg/g)	11.303	9.596	9.606	6.983	6.798
	R2	0.9498	0.9888	0.9823	0.9786	0.992
Experimental	Parameters	Ca <sup>2+</sup>	Mn <sup>2+</sup>	Fe <sup>3+</sup>	Mg <sup>2+</sup>	Pb <sup>2+</sup>
	qe Exp.(mg/g)	7	7	7	7	7

The results showed that the pseudo-2<sup>nd</sup>-order model, with its stronger correlation coefficient R2 and qe values that are closer to the experimental values, generates more straight lines than the pseudo-1<sup>st</sup>-order model. This proves that electron transfer between the adsorbate and the adsorbent surface is the primary mechanism at play (chemisorption). Typically, just one layer of molecules may be chemisorbed onto an adsorbent's surface (El Qada *et al.*, 2006).

**Equilibrium Parameters of the Adsorption**

Adsorption isotherms (Ghoniem *et al.*, 2014).are mathematical models that explain the behavior of adsorbate species in both liquid and solid phases. The adsorption isotherm was analyzed at a constant temperature of 25°C and for a range of ion concentrations. Cation adsorption equilibrium findings were analyzed

using Freundlich and Langmuir isotherm models for illite and nanoillite (Tables 3 and 4).

Langmuir isotherm models, which assume a uniform surface, assume that just a single adsorption monolayer occurs on an adsorbent. When the metal ions are evenly distributed across the solid and liquid phases, a monolayer occurs. When a monolayer of the adsorbate forms on the surface of the adsorbent, further adsorption ceases (Shama *et al.*, 2010).

Figure 6 show Langmuir models for the ions by charting Ce/q<sub>c</sub> against Ce. The maximum monolayer adsorption capacity, q<sub>max</sub>, was calculated from the slope, whereas the dissociation constant, K<sub>L</sub>, was determined from the intercept (Meshram *et al.*, 2012).

Freundlich isotherm models (Figure 7) are purely empirical and provide the best description of adsorption on heterogeneous surfaces. (Freundlich, 1906)

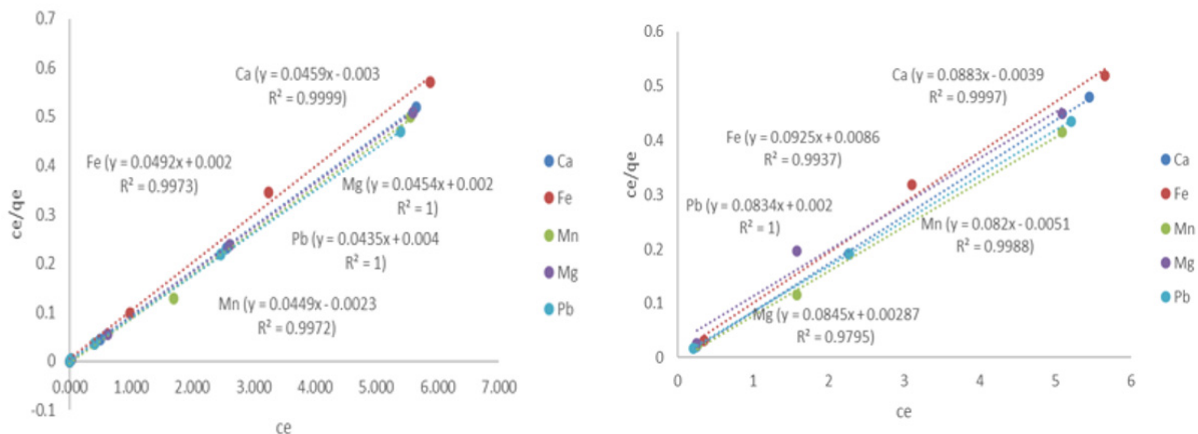


**Figure 6:** Langmuir isotherm model on illite and nano illite

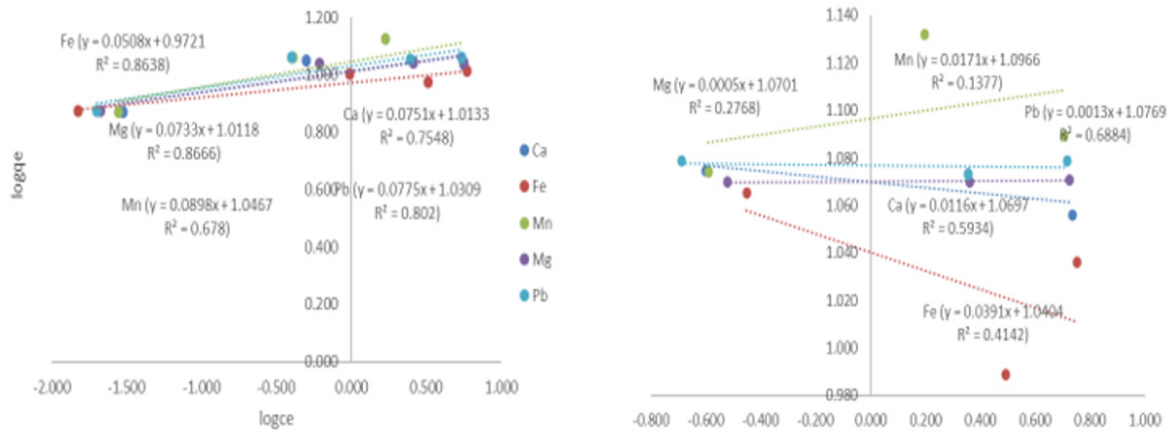


Figure 7: Freundlich isotherm model on illite and nano illite

Table 3: Calculated isotherm parameters on illite

Langmuir	Parameters	Ca <sup>2+</sup>	Mn <sup>2+</sup>	Fe <sup>3+</sup>	Mg <sup>2+</sup>	Pb <sup>2+</sup>
	kL (L/mg)	15.30	19.52	24.59	22.69	10.87
qmax mg/g)	21.78	22.27	20.33	22.03	22.99	
RL	0.006	0.005	0.004	0.004	0.009	
R2	0.9999	0.9972	0.9973	1	1	
Freundlich	kf (L/g)	10.31	11.41	9.37	10.27	10.73
	1/n	0.0751	0.0898	0.0508	0.0733	0.0775
	R2	0.7548	0.678	0.863	0.8666	0.802

Table 4: Calculated isotherm parameters on nano illite

Langmuir	Parameters	Ca <sup>2+</sup>	Mn <sup>2+</sup>	Fe <sup>3+</sup>	Mg <sup>2+</sup>	Pb <sup>2+</sup>
	kL (L/mg)	22.63	16.08	10.75	29.45	41.70
qmax mg/g)	11.33	12.19	10.81	11.83	11.99	
RL	0.004	0.006	0.009	0.003	0.002	
R2	0.9997	0.9988	0.9937	0.9795	1	
Freundlich	kf (L/g)	11.74	12.49	10.97	11.75	11.93
	1/n	0.0116	0.0171	0.0391	0.0005	0.0013
	R2	0.5934	0.1377	0.4141	0.2768	0.6884

Since  $R_L$  is greater than 0 and less than 1, the results support the Langmuir model's prediction of success. Since  $1/n$  is larger than 0.1 and less than unity, the Freundlich model predicts favorability as  $1/n$ . The investigated metal ion processes are consistent with the Langmuir isotherm model (Shama *et al.*, 2010), even though the Langmuir model has a lower  $R_2$  value than the Freundlich model.

#### Application to Real Underground Water

To evaluate the efficacy of a treatment method for removing Ca (II), Mn(II), Fe(III), Mg(II), and Pb(II)-ions from synthetic water, a sample of subsurface water from the Egyptian city of El-Kharga was collected. The material was filtered via a filter with a 0.45- $\mu$ m membrane. A flame atomic absorption spectrophotometer determined

Table 5: Adsorption of metal cations from underground water using illite and nano illite

Metal ions	Concentration (mg/L) before treatment	Concentration (mg/L) After treatment		Removal percentage %	
		illite	nano-illite	illite	nano-illite
Cu(II)	3.541	-	-	100%	100%
Mn(II)	0.97	-	-	100%	100%
Fe(III)	4.22	-	-	100%	100%
Cd(II)	0.2132	-	-	100%	100%
Pb(II)	0.6143	-	-	100%	100%
Ca(II)	67.3	6.73	-	90%	100%
Mg(II)	31.8	4.77	-	85%	100%

a water sample's metal content. The optimal treatment parameters for removing Ca (II), Mn (II), Fe (III), Mg (II), and Pb (II) ions from synthetic water were found to be pH = 7, adsorbent dosage = 0.4g, and contact duration = 1h, according to batch experimental data.

Each adsorbent was used in a mixture of 50 mL of water in the experiment. The mixture was held at pH 7 and 25 °C for 90 minutes at 500 rpm. Suspensions were filtered using 0.45 m membrane filter paper and stored for further metal analysis.

## CONCLUSION

Lack of access to modern water treatment procedures that would eliminate heavy metal pollution of water sources like groundwater is an increasing problem in developing nations. Thus, there is an intensive study into the utilization of inexpensive adsorbents for the elimination of heavy materials.

Groundwater refers to water extracted from aquifers, which is water located in subterranean voids or fractures in sediments and is used for human use. Because it helps our natural environment persist, it plays a crucial role in our day-to-day lives.

Ca (II), Mn (II), Fe (III), Mg (II), and Pb ion removal were studied in illite and nano-illite (II). Different contact times, initial concentrations, adsorbent dosages, and pH values were tested in batch adsorption experiments. Results showed that at pH 7, adsorption capabilities for all metal ions studied were at their highest. Adsorbent doses up to 0.4 g were effective. Metal removal for all ions approached equilibrium after 60 minutes. Monolayer chemisorption of metal ions on illite and nano-illite particles is described by the Langmuir and pseudo-2<sup>nd</sup>-order kinetic models. The shrinkage of clay particles to the nanoscale has the potential to greatly boost their ability to operate as adsorbents because of clay's enormous surface area and distinctive charge. It is possible that efficient and inexpensive adsorbents may be made by combining the properties of natural clay with those of nanoparticles.

## REFERENCES

Anjum, M., Miandad, R., Waqas, M., Gehany, F., & Barakat, M. A. (2019). Remediation of wastewater using various nano-materials. *Arabian Journal of Chemistry*, 12(8), 4897–4949.

Burakov, A. E., Galunin, E. V., Burakova, I. V., Kucherova, A. E., Agarwal, S., Tkachev, A. G., & Gupta, V. K. (2018). Adsorption of heavy metals on conventional and nanostructured materials for wastewater treatment purposes: A review. *Ecotoxicology and Environmental Safety*, 148, 702–712.

El Qada, E. N., Allen, S. J., & Walker, G. M. (2006). Adsorption of methylene blue onto activated carbon produced from steam activated bituminous coal: A study of equilibrium adsorption isotherm. *Chemical Engineering Journal*, 124, 103–110.

Freundlich, H. M. F. (1906). Über die adsorption in lösungen. *Zeitschrift für Physikalische Chemie*, 57, 385–470.

Ghoniem, M. M., El-Desoky, H. S., El-Moselhy, K. M., Amer, A., AboEl-Naga, E. H., Mohamedein, L. I., & Al-Prol, A. E. (2014). Removal of cadmium from aqueous solution using green marine algae, *Ulva lactuca*.

Hoang, A. T., Nizetić, S., Cheng, C. K., Luque, R., Thomas, S., Banh, T. L., VietPham, V., & Nguyen, X. P. (2022). Heavy metal removal by biomass-derived carbon nanotubes as a greener environmental remediation: A comprehensive review. *Chemosphere*, 287, 131959.

Hoang, H. G., Chiang, C. F., Lin, C., Wu, C. Y., Lee, C. W., Cheruiyot, N. K., Tran, H. T., & Bu, X. T. (2021). Human health risk simulation and assessment of heavy metal contamination in a river affected by industrial activities. *Environmental Pollution*, 285, 117414.

Ishwah, B., Kukwa, R. E., Ajegi, J. O., Samoh, T. F., Iortile, T. M., Ngunoon, T. P., Igbawase, S. D., & Nyerere, A. C. (2022). Adsorption of Some Heavy Metals from Wastewater using Fine Sand and Zeolite. *American Journal of Chemistry and Pharmacy*, 1(1), 11–17. <https://doi.org/10.54536/ajcp.v1i1.385>

Jawed, A., Saxena, V., & Pandey, L. M. (2020). Engineered nanomaterials and their surface functionalization for the removal of heavy metals: A review. *Journal of Water Process Engineering*, 33, 101009.

Joiziane, G. M., Murilo, P. M., Thirugnanasambandham, K., Sergio, H. B. F., Marcelino, L. G., Maria, A. S. D. B., & Sivakumar, V. (2017). Preparation and characterization of calcium treated bentonite clay and its application for the removal of lead and cadmium ions: Adsorption and thermodynamic modeling. *Process Safety and Environmental Protection*, 111(2017), 244–252.

Kwon, J. S., Yun, S. T., Lee, J. H., Kim, S. O., Jo, H. Y. (2010). Removal of divalent heavy metals (Cd, Cu, Pb, and Zn) and arsenic(III) from aqueous solutions using scoria: kinetics and equilibria of sorption. *Journal of Hazardous Materials*, 174(1-3), 307-13. <https://doi.org/10.1016/j.jhazmat.2009.09.052>.

Langmuir, I. (1918). The adsorption of gases on plane surfaces of glass, mica and platinum. *Journal of the American Chemical Society*, 40, 1361–1403.

Lee, I., Park, C. W., Yoon, S. S., & Yang, H. M. (2019). Facile synthesis of copper ferrocyanide-embedded magnetic hydrogel beads for the enhanced removal of cesium from water. *Chemosphere*, 224, 776–785.

Li, C., Wang, H., Liao, X., Xiao, R., Liu, K., Bai, J., Li, B., & He, Q. (2022). Heavy metal pollution in coastal wetlands: A systematic review of studies globally over the past three decades. *Journal of Hazardous Materials*, 424, 127312.

Liu, W., Wang, D., Soomro, R. A., Fu, F., Qiao, N., Yu, Y., Wang, R., & Xu, B. (2019). Ceramic supported attapulgite-graphene oxide composite membrane for efficient removal of heavy metal contamination. *Journal of Membrane Science*, 591, 117323.

Mohammad, K. U. (2017). A review on the adsorption of heavy metals by clay minerals, with special focus

- on the past decade. *Chemical Engineering Journal*, 308, 438–462.
- Meshram, P., Sahu, S. K., Pandey, P. D., Kumar, V., & Mankhand, T. R. (2012). Removal of chromium(II) from the waste solution of an Indian Tannery by Amberlite IR 120 Resin. *International Journal of Nonferrous Metallurgy*, 1, 32-41.
- Mhina, C. F., Jung, H. Y., & Kim, J. K. (2020). Recovery of antioxidant and antimicrobial peptides through the reutilization of Nile perch wastewater by biodegradation using two *Bacillus* species. *Chemosphere*, 253, 126728.
- Ngulube, T., Gumbo, J. R., Masindi, V., & Maity, A. (2017). An update on synthetic dyes adsorption onto clay-based minerals: A state-of-the-art review. *Journal of Environmental Management*, 191, 35–57.
- Peng, W., Li, H., Liu, Y., Song, S. (2017). A review on heavy metal ions adsorption from water by graphene oxide and its composites. *Journal of Molecular Liquids*, 230, 496–504.
- Sari, A., & Tuzen, M. (2014). Cd(II) adsorption from aqueous solution by raw and modified kaolinite. *Applied Clay Science*, 88–89, 63–72.
- Sen, T. K., & Gomez, D. (2011). Adsorption of zinc (Zn<sup>2+</sup>) from aqueous solution on natural bentonite. *Desalination*, 267, 286-294.
- Shama, S. A., & Gad, M. A. (2010). Removal of heavy metals (Fe<sup>3+</sup>, Cu<sup>2+</sup>, Zn<sup>2+</sup>, Pb<sup>2+</sup>, Cr<sup>3+</sup>, and Cd<sup>2+</sup>) from aqueous solutions by using hebbra clay and activated carbon. *Journal of Portugaliae Electrochimica Acta*, 28, 231-239.
- Silva, S. P., Sousa, S., & Rodrigues, J. (2004). Adsorption of Acid Orange 7 Dye in Aqueous Solutions by Spent Brewery Grains. *Journal of Separation and Purification Technology*, 40, 309–315.
- Wadhawan, S., Jain, A., Nayyar, J., & Mehta, S. K. (2020). Role of nanomaterials as adsorbents in heavy metal ion removal from wastewater: A review. *Journal of Water Process Engineering*, 33, 101038.
- Yuan, S. S., Li, Z. Y., Pan, Z. D., & Wang, Y. M. (2016). Removal of Copper and Cadmium Ions in Aqueous Solution via Adsorption by Nano-sized Illite-Smectite Clay. *Journal of the Chinese Ceramic Society*, 44, 43–49.
- Zaynab, M., Al-Yahyai, R., Ameen, A., Sharif, Y., Ali, L., Fatim, M., AliKhan, K., & Li, S. (2022). Health and environmental effects of heavy metals. *Journal of King Saud University - Science*, 34, 101653.
- Zhang, L. H., Yuan, Y. H., Yan, Z. G., Zhou, Y. Y., Zhang, C. Y., Huang, Y., & Xu, M. (2016). Application of nano illite/smectite clay for adsorptive removal of metals in water. *Research in Environmental Science*, 29, 115–123.
- Zhang, X., Dou, Y., Gao, C., He, C., Gao, J., Zhao, S., & Deng, L. (2019). Removal of Cd(II) by modified maifanite coated with Mg-layered double hydroxides in constructed rapid infiltration systems. *Science of The Total Environment*, 685, 951–962.
- Zhao, Y., Kang, S., Qin, L., Wang, W., Zhang, T., Song, S., & Komarneni, S. (2020). Self-assembled gels of Fe-chitosan/montmorillonite nanosheets: Dye degradation by the synergistic effect of adsorption and photo-Fenton reaction. *Chemical Engineering Journal*, 379, 122322.